Report

Neuron

Estrogens Suppress a Behavioral Phenotype in Zebrafish Mutants of the Autism Risk Gene, *CNTNAP2*

Highlights

- Zebrafish mutants of the autism risk gene *cntnap2* have GABAergic neuron deficits
- High-throughput behavioral profiling identifies nighttime hyperactivity in mutants
- *cntnap2* mutants exhibit altered responses to GABAergic and glutamatergic compounds
- Estrogenic compounds suppress the *cntnap2* mutant behavioral phenotype

Authors

Ellen J. Hoffman, Katherine J. Turner, Joseph M. Fernandez, ..., Jason Rihel, Matthew W. State, Antonio J. Giraldez

Correspondence

j.rihel@ucl.ac.uk (J.R.), matthew.state@ucsf.edu (M.W.S.), antonio.giraldez@yale.edu (A.J.G.)

In Brief

Hoffman et al. use zebrafish mutants of the autism risk gene *Contactin Associated Protein-like 2* (*CNTNAP2*) to conduct high-throughput quantitative behavioral profiling and pharmacological screening. This approach reveals dysregulation of GABAergic and glutamatergic systems in mutants and identifies estrogenic compounds as suppressors of the mutant behavioral phenotype.

Accession Numbers

KU376408
KU376409

Hoffman et al., 2016, Neuron *89*, 725–733
February 17, 2016 ©2016 Elsevier Inc.
http://dx.doi.org/10.1016/j.neuron.2015.12.039

CellPress

Neuron
Report

Estrogens Suppress a Behavioral Phenotype in Zebrafish Mutants of the Autism Risk Gene, *CNTNAP2*

Ellen J. Hoffman,[1,2] Katherine J. Turner,[3] Joseph M. Fernandez,[1,2] Daniel Cifuentes,[4,5] Marcus Ghosh,[3] Sundas Ijaz,[1,2] Roshan A. Jain,[6,7] Fumi Kubo,[8] Brent R. Bill,[9,10] Herwig Baier,[8] Michael Granato,[6] Michael J.F. Barresi,[11] Stephen W. Wilson,[3] Jason Rihel,[3,*] Matthew W. State,[1,2,4,12,*] and Antonio J. Giraldez[4,*]

[1]Child Study Center
[2]Program on Neurogenetics
Yale School of Medicine, New Haven, CT 06510, USA
[3]Department of Cell and Developmental Biology, University College London, Gower Street, London WC1E 6BT, UK
[4]Department of Genetics, Yale University School of Medicine, New Haven, CT 06510, USA
[5]Department of Biochemistry, Boston University School of Medicine, Boston, MA 02118, USA
[6]Department of Cell and Developmental Biology, University of Pennsylvania, Perelman School of Medicine, Philadelphia, PA 19104, USA
[7]Department of Biology, Haverford College, Haverford, PA 19041, USA
[8]Department Genes - Circuits - Behavior, Max Planck Institute of Neurobiology, Am Klopferspitz 18, 82152 Martinsried, Germany
[9]Center for Autism Research and Treatment, Semel Institute for Neuroscience and Human Behavior, Department of Psychiatry, University of California, Los Angeles, Los Angeles, CA 90095, USA
[10]Department of Biology, The University of Texas at Tyler, Tyler, TX 75799, USA
[11]Department of Biological Sciences, Smith College, Northampton, MA 01063, USA
[12]Department of Psychiatry, University of California, San Francisco, San Francisco, CA 94143, USA
*Correspondence: j.rihel@ucl.ac.uk (J.R.), matthew.state@ucsf.edu (M.W.S.), antonio.giraldez@yale.edu (A.J.G.)
http://dx.doi.org/10.1016/j.neuron.2015.12.039

SUMMARY

Autism spectrum disorders (ASDs) are a group of devastating neurodevelopmental syndromes that affect up to 1 in 68 children. Despite advances in the identification of ASD risk genes, the mechanisms underlying ASDs remain unknown. Homozygous loss-of-function mutations in *Contactin Associated Protein-like 2* (*CNTNAP2*) are strongly linked to ASDs. Here we investigate the function of Cntnap2 and undertake pharmacological screens to identify phenotypic suppressors. We find that zebrafish *cntnap2* mutants display GABAergic deficits, particularly in the forebrain, and sensitivity to drug-induced seizures. High-throughput behavioral profiling identifies nighttime hyperactivity in *cntnap2* mutants, while pharmacological testing reveals dysregulation of GABAergic and glutamatergic systems. Finally, we find that estrogen receptor agonists elicit a behavioral fingerprint anti-correlative to that of *cntnap2* mutants and show that the phytoestrogen biochanin A specifically reverses the mutant behavioral phenotype. These results identify estrogenic compounds as phenotypic suppressors and illuminate novel pharmacological pathways with relevance to autism.

INTRODUCTION

Autism spectrum disorders (ASDs) are a group of neurodevelopmental syndromes characterized by deficits in social interaction and communication as well as repetitive behaviors and restricted interests (American Psychiatric Association, 2013). Gene discovery in ASDs has accelerated dramatically (De Rubeis et al., 2014; Iossifov et al., 2014; Sanders et al., 2015), providing a launching point for the illumination of relevant biological pathways (Pariksh ak et al., 2013; Willsey et al., 2013). *Contactin Associated Protein-like 2* (*CNTNAP2*) is one of the first genes strongly linked to autism and epilepsy in consanguineous families (Strauss et al., 2006). This gene encodes a cell adhesion molecule of the neurexin family that localizes voltage-gated potassium channels at the juxtaparanodal region of myelinated axons (Poliak et al., 2003). Loss of CNTNAP2 function in mice leads to abnormal neuronal migration, reduced GABAergic neurons, spontaneous seizures, hyperactivity, social deficits, and increased repetitive behaviors (Peñagarikano et al., 2011). However, the function of CNTNAP2 in the CNS and the consequences of its loss for ASD pathology are less well understood.

At present, our ability to advance rapidly from the identification of risk genes to the discovery of biological mechanisms and pharmacological suppressors remains limited. The zebrafish is a model vertebrate system well suited for conducting small molecule screens to uncover modulators of signaling pathways (Ablain and Zon, 2013; Kokel and Peterson, 2011; Rihel et al., 2010). Quantitative behavioral profiling provides a high-throughput approach to characterize psychoactive molecules

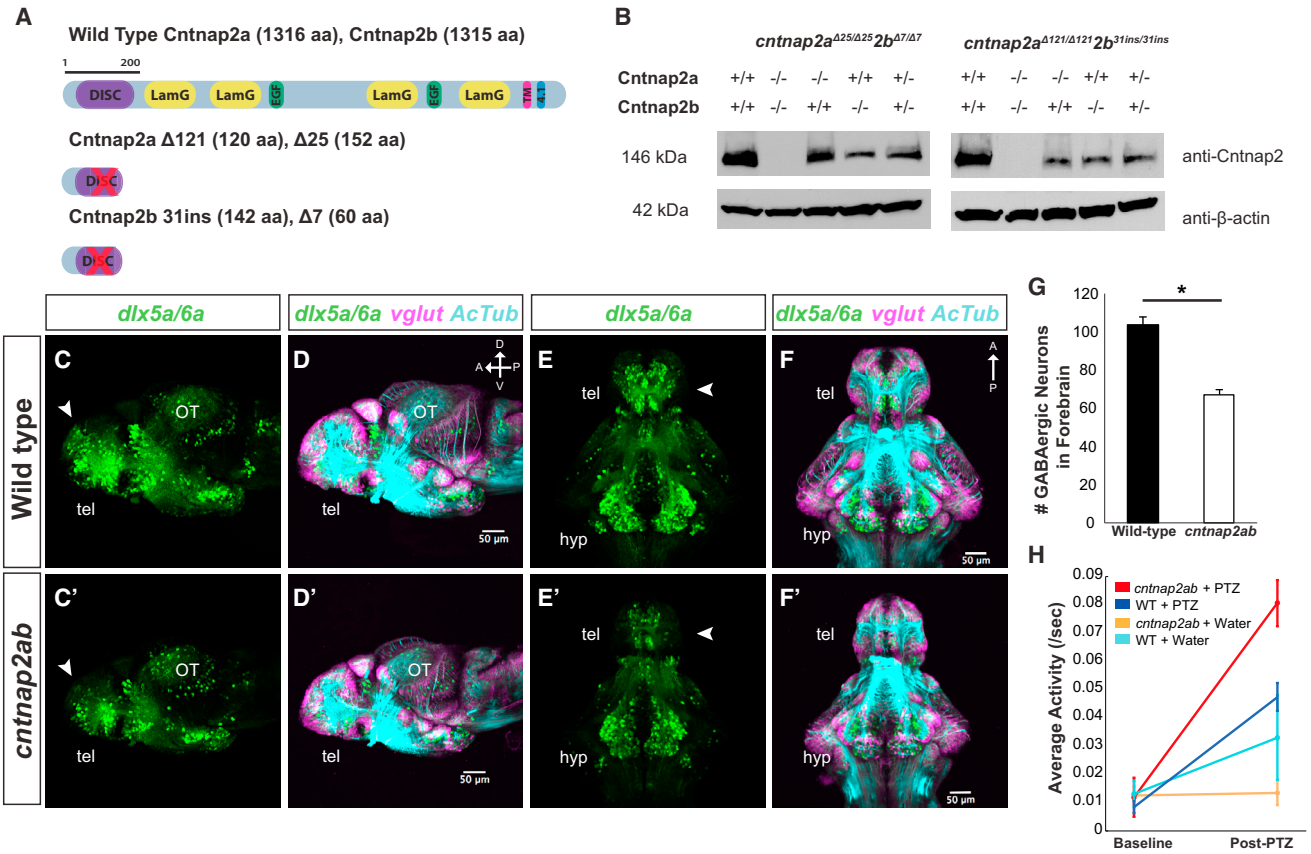

Figure 1. *cntnap2ab* Mutants Display GABAergic Deficits

(A) Cntnap2a and Cntnap2b proteins showing functional domains. DISC, discoidin; EGF, epidermal growth factor; 4.1, 4.1 binding domain; LamG, laminin G; TM, transmembrane.

(B) Western blot analysis of Cntnap2a and Cntnap2b in *cntnap2a*$^{\Delta25/\Delta25}$*cntnap2b*$^{\Delta7/\Delta7}$ and *cntnap2a*$^{\Delta121/\Delta121}$*cntnap2b*$^{31i/31i}$ fish.

(C–F and C′–F′) Reporter gene expression in Tg(*dlx6a-1.4kbdlx5a/dlx6a:GFP*) and Tg(*vglut:DsRed*) in wild-type (C–F) and *cntnap2a*$^{\Delta121/\Delta121}$*cntnap2b*$^{31i/31i}$ (*cntnap2ab*) (C′–F′) larvae at 4 dpf. Note the deficit in *dlx5a/6a*:GFP+ cells in the telencephalon (arrowheads). (C and D, C′ and D′) Lateral views. (E and F, E′ and F′) Ventral views. hyp, hypothalamus; OT, optic tectum; tel, telencephalon.

(G) Total number of *dlx5a/6a*:GFP+ cells in the forebrain of wild-type (n = 13) and *cntnap2ab* mutants (n = 14). *p = 3.08 × 10^{-7} (one-way ANOVA).

(H) Average activity in response to PTZ (10 mM) in the progeny of incrossed *cntnap2a*$^{\Delta25/+}$*cntnap2b*$^{\Delta7/+}$ fish at 4 dpf (n = 268; *cntnap2ab* + PTZ, n = 6; wild-type + PTZ, n = 11; *cntnap2ab* + water, n = 11; wild-type + water, n = 6; p = 0.0013, two-way ANOVA, genotype × dose interaction).

on the basis of the behavioral readout of their effects in zebrafish larvae (Rihel et al., 2010). Here we investigate the consequences of the loss of Cntnap2 in zebrafish and use quantitative behavioral profiling as a platform to conduct rational pharmacological screens to identify phenotypic suppressors and novel pathways with relevance to autism.

RESULTS

cntnap2 Mutants Display GABAergic Deficits

Zebrafish have two *cntnap2* paralogs that are expressed broadly in the developing CNS, with higher expression in the telencephalon (Figures S1A–S1C). Cntnap2a and Cntnap2b proteins show 71% and 65% identity to the human protein, respectively, and contain the same functional domains (Figure 1A). To characterize their function, we generated two loss-of-function mutations in each paralog using zinc finger nucleases and crossed fish carrying these alleles to generate double-mutant fish (*cntnap2a*$^{\Delta121/\Delta121}$*cntnap2b*$^{31i/31i}$ and *cntnap2a*$^{\Delta25/\Delta25}$*cntnap2b*$^{\Delta7/\Delta7}$) (Figures S1D–S1F), referred to hereafter as *cntnap2ab* mutants. Each mutation causes a premature stop codon within the discoidin domain and results in loss of protein expression (Figures 1A and 1B), such that double mutants represent a loss of Cntnap2 function.

It has been proposed that an imbalance in excitatory and inhibitory signaling in the CNS is a mechanism underlying ASD and epilepsy (Rubenstein and Merzenich, 2003). To test if this is occurring in *cntnap2ab* mutants, we analyzed inhibitory and excitatory neuronal populations in wild-type and *cntnap2ab* mutants during early brain development, using transgenic lines that label GABAergic neurons and precursors (Tg[*dlx6a-1.4kbdlx5a/dlx6a:GFP*]) and glutamatergic neurons (Tg[*vglut:DsRed*]) (Ghanem et al., 2003; Kinkhabwala et al., 2011; Zerucha et al., 2000). We observed a significant decrease in GABAergic cells

in *cntnap2ab* mutants at 4 days post fertilization (dpf) (Figures 1C–1F, 1C′–1F′, S2A–S2H, and S2A′–S2H′) in the forebrain and cerebellum (Figures S2I and S2J). In particular, there was an average of 34% fewer GABAergic neurons in the forebrain of *cntnap2ab* mutants compared with wild-type fish at 4 dpf (Figure 1G; $p = 3.08 \times 10^{-7}$, one-way ANOVA). The decreased number of GABAergic cells in the dorsal telencephalon (pallium) at this stage is consistent with a failure in the migration of these cells from the ventral telencephalon (subpallium), similar to findings reported in *Cntnap2* mutant mice (Peñagarikano et al., 2011). In contrast, there were no significant regional deficits in glutamatergic neurons (Figures S2A–S2H, S2A′–S2H′, and S2K).

Although there were no gross morphological abnormalities in the structure of the axon scaffold in *cntnap2ab* mutants between 48 hr post fertilization (hpf) and 5 dpf (Figures S1H, S2I, S1H′, and S2I′), mutant head size is significantly smaller (Table S1; Figures S1N–S1R and S1N′–S1Q′). In addition, we did not observe gross differences in markers of apoptosis (TUNEL staining) at 28 hpf or proliferation (phospho-histone H3) at 48 hpf (Figures S2R, S2S, S2R′, and S2S′). However, deficits in GABAergic neurons and transient delays in commissure formation are evident in the forebrain of mutants at 28 hpf (Figures S1J–S1M, S1J′, and S1K′), indicating additional early roles for Cntnap2 in brain development. Together, these data indicate loss of Cntnap2 results in a deficit of inhibitory neurons, particularly in the forebrain.

Increased Seizure Susceptibility in *cntnap2* Mutants

Loss of inhibitory neurons can increase susceptibility to seizures (Cobos et al., 2005). To determine the effect of loss of Cntnap2 on seizure susceptibility in zebrafish, we treated wild-type and mutant larvae with pentylenetetrazol (PTZ), a GABA-A receptor antagonist that induces seizures in rodents and zebrafish (Baraban et al., 2005; Watanabe et al., 2010). *cntnap2ab* mutants display increased sensitivity to PTZ-induced seizures (Figures 1H and S3A–S3F). Drug-induced seizures appear as robust increases in activity and rapid, burst-like and circling movements, followed by periods of inactivity (Baraban et al., 2005). Homozygous double mutants display significantly more activity in response to PTZ (Figure S4B; $p = 0.0013$, two-way ANOVA, genotype × dose interaction, $n = 268$). These results are consistent with increased seizures associated with *CNTNAP2* mutations in humans and mice (Peñagarikano et al., 2011; Strauss et al., 2006). Consequently, increased sensitivity to PTZ provides further evidence for GABAergic deficits in *cntnap2ab* mutants.

cntnap2 Mutants Show Nighttime Hyperactivity

We next adapted a blinded, high-throughput assay to quantify a series of rest-wake cycle behavioral parameters over multiple days (Figure 2A) (Prober et al., 2006; Rihel et al., 2010). Quantitative profiling revealed that *cntnap2ab* mutants display significantly greater nighttime activity compared with wild-type siblings between 4 and 7 dpf (Figures 2B, 2C, and S3G; $p = 0.00012$, one-way ANOVA, $n = 838$). This phenotype was independently observed in *cntnap2ab* mutants harboring different alleles (Figure S3H; $p = 0.0198$, $n = 187$). In contrast, other rest-wake parameters (Table S2), as well as acoustic startle, habituation, and optokinetic response (Table S3), were not significantly affected, further highlighting the specificity of the nighttime hyperactivity phenotype. Combined, these results indicate that loss of Cntnap2 selectively causes nighttime hyperactivity, consistent with GABAergic deficits leading to an imbalance of excitatory and inhibitory signaling in mutant fish.

Differential Responses to Psychoactive Agents in *cntnap2* Mutants

Collectively, the day-night, rest-wake cycle parameters of *cntnap2ab* mutants represent a behavioral fingerprint with a specific nighttime hyperactivity signature. To identify molecular pathways that are dysregulated in the absence of Cntnap2 function, we searched for drugs that phenocopy the mutant behavioral profile. To this end, we compared the *cntnap2ab* mutant behavioral fingerprint with a data set of the behavioral profiles of wild-type larvae exposed to 550 psychoactive compounds (Rihel et al., 2010). This allowed an unbiased comparison of the different genetic and pharmacological conditions by cluster analysis (Rihel et al., 2010) (Figure 2D) and resulted in the identification of small molecules that strongly correlate with the mutant behavioral profile (Figure 2E). Next, we identified the top 14 drugs that anti-correlate, or generate the opposite phenotype of the mutant behavioral profile (Figure S4H). We reasoned that drugs that induce differential effects in wild-type and mutant larvae might indicate pathways that are dysregulated because of loss of Cntnap2. To test this, we exposed wild-type and *cntnap2a*$^{\Delta 121/\Delta 121}$*cntnap2b*$^{31i/31i}$ larvae to a group of compounds from 4–7 dpf (Figure 3A) that were selected on the basis of the following criteria: (1) correlating; (2) anti-correlating; (3) GABA-A receptor agonists, based on the structural GABAergic deficits; and (4) risperidone, because it is the first U.S. Food and Drug Administration-approved treatment for irritability and aggressive behavior in ASDs (McCracken et al., 2002).

Three lines of evidence indicate that both glutamatergic and GABAergic pathways are dysregulated in *cntnap2ab* mutants. First, we found that both GABA- and NMDA-receptor antagonists are significantly enriched among drugs that strongly correlate with the mutant phenotype (Figures 3D and 3E; $p = 0.031$ and $p = 0.034$, respectively, Kolmogorov-Smirnov test). These findings are consistent with the behavioral profile of *cntnap2ab* mutants, given that NMDA receptor antagonists induce nighttime hyperactivity in wild-type larvae, and the increased sensitivity of mutants to the GABA-A receptor antagonist, PTZ. Second, *cntnap2ab* mutants are more sensitive to arousal by NMDA receptor antagonists across a range of doses (Figure 3B), suggesting attenuation of glutamatergic signaling.

Third, we found that GABA receptor agonists, such as zolpidem, induce differential behavioral effects in *cntnap2ab* mutants compared to wild-type larvae (Figures 3C and 3F–3H). For this analysis, we performed hierarchical clustering and principal-component analysis (PCA) to quantify differential mutant responses compared with wild-type across 18 rest-wake activity parameters (Rihel et al., 2010). Specifically, we calculated the Euclidean distance between the mutant + drug and wild-type + drug behavioral profiles, representing the difference between the mutant and wild-type responses to each drug (Figures 3H and S4A–S4F; see Supplemental Experimental Procedures).

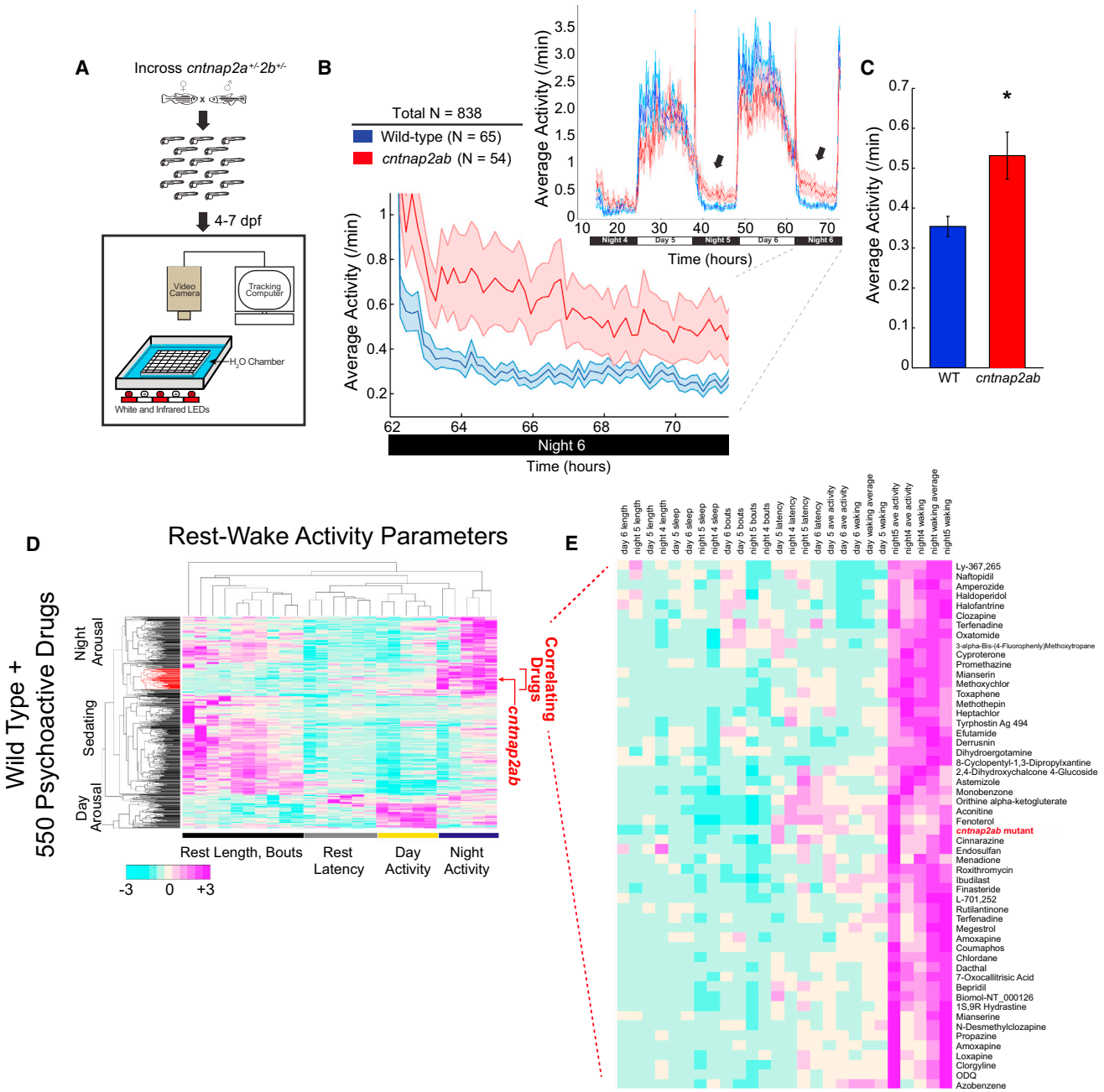

Figure 2. *cntnap2ab* Mutants Display Nighttime Hyperactivity

(A) Experimental setup (Prober et al., 2006; Rihel et al., 2010).

(B) Locomotor activity of *cntnap2a*$^{\Delta 25/\Delta 25}$*cntnap2b*$^{\Delta 7/\Delta 7}$ (*cntnap2ab*, red) and wild-type (WT; blue) sibling-matched larvae over 72 hr. Hyperactivity in mutants worsens on successive nights (arrows). The magnified activity profile on night 6 is shown.

(C) Average locomotor activity of *cntnap2ab* versus wild-type. *p = 0.00012 (one-way ANOVA, comparing all genotypes on all nights); p = 0.0193, 0.0236, and 0.0073, nights 4, 5, and 6, respectively.

(D) Hierarchical clustering of the *cntnap2ab* behavioral fingerprint (red arrow) compared with the fingerprints of wild-type larvae exposed to a panel of 550 psychoactive agents from 4–6 dpf (Rihel et al., 2010). Each rectangle in the clustergram represents the *Z* score, or the average value in SDs relative to the behavioral profiles of wild-type exposed to DMSO alone (magenta, higher than DMSO; cyan, lower than DMSO). The *cntnap2ab* profile correlates with agents that induce nighttime arousal ("Correlating Drugs").

(E) A magnified section of the clustergram, highlighting compounds that correlate with the *cntnap2ab* mutant behavioral fingerprint.

A

Psychoactive Drugs Tested

Compound Name	Biological Target(s)	Rationale for Selection
L-701,324	NMDA glycine site antagonist	Correlating
(-)-MK-801	Non-competitive NMDA receptor antagonist	Correlating
Amantadine	Dopaminergic; increases dopamine synthesis/release, inhibits reuptake	Anti-Correlating
(+)-Baclofen	GABA-B receptor agonist	Anti-Correlating
β-Estradiol	Estrogen receptor-β agonist	Anti-Correlating
β-Estradiol 17-cypionate	Estrogen receptor-β agonist	Anti-Correlating
Biochanin A	Estrogen receptor-β agonist	Anti-Correlating
CGS-12066	5HT1B serotonin receptor agonist	Anti-Correlating
Chlorzoxazone	Centrally acting muscle relaxant	Anti-Correlating
Clonidine	α2-adrenergic receptor agonist	Anti-Correlating
Ticlopidine	Platelet aggregation inhibitor	Anti-Correlating
Risperidone	Dopamine (D2) and serotonin (5-HT2A) receptor antagonist	FDA-approved for irritability in ASD
Zolpidem	Nonbenzodiazepine GABA-A receptor agonist	GABAergic deficit
Diazepam	Benzodiazepine; positive allosteric GABA-A receptor modulator	GABAergic deficit

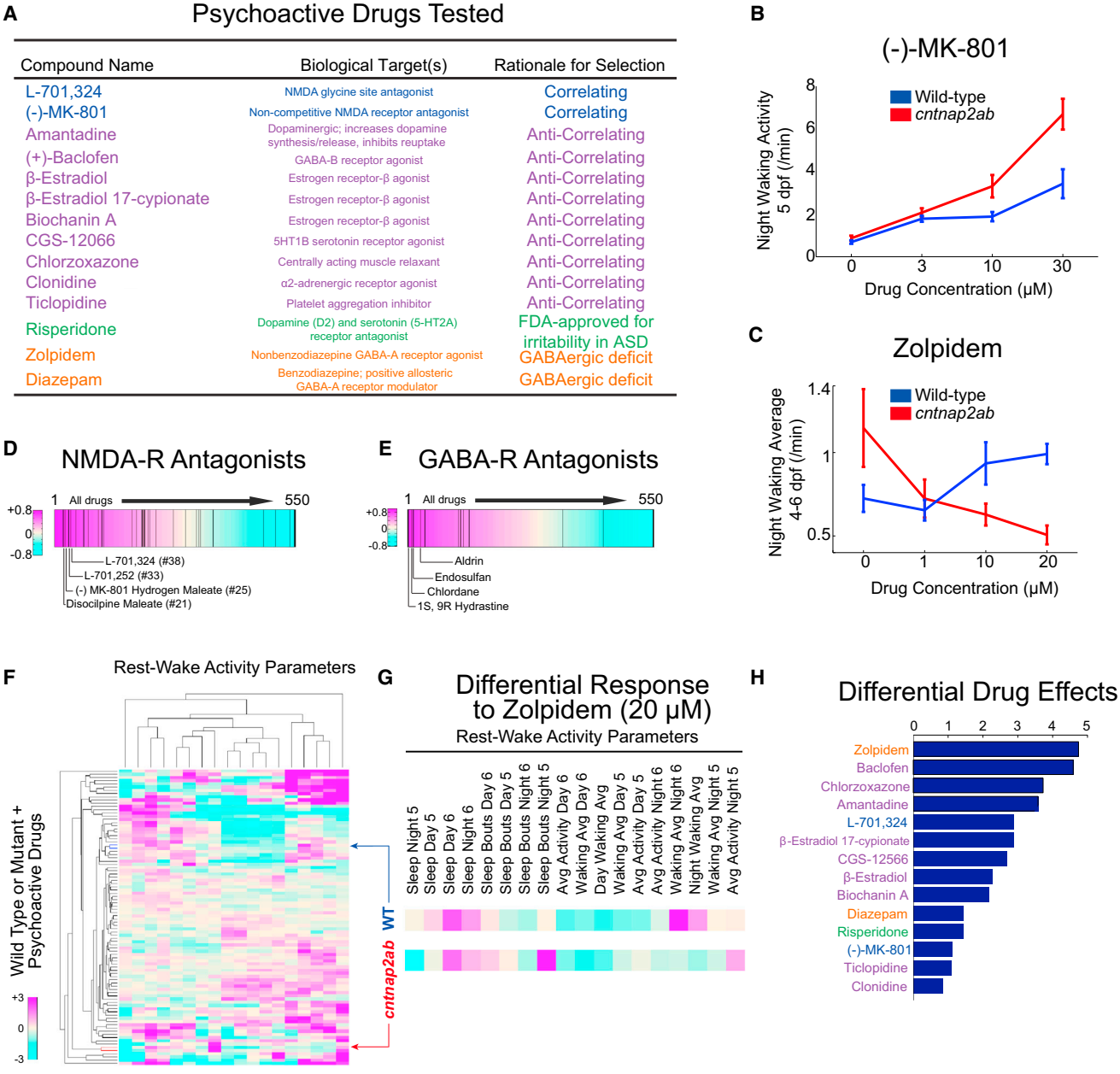

Figure 3. Differential Behavioral Responses of *cntnap2ab* Mutants to Psychoactive Agents

(A) The 14 psychoactive drugs tested in *cntnap2a*$^{\Delta121/\Delta121}$*cntnap2b*$^{31i/31i}$ and wild-type larvae, their biological targets, and the rationale for their selection. The following classes of drugs are shown: correlating (blue), anti-correlating (purple), drugs interacting with the GABA-A receptor (orange), and risperidone (green).

(B and C) Dose-response effects of the NMDA receptor antagonist, (-)-MK-801, on night waking activity at 5 dpf (B) and the non-benzodiazepine GABA-A receptor agonist zolpidem on average night waking activity at 4–6 dpf (C) in wild-type (WT; blue) and *cntnap2ab* (red) larvae ($p = 0.002$, (-)-MK-801; $p = 0.0003$, zolpidem; two-way ANOVA, genotype × drug interaction).

(D and E) Significant enrichment of NMDA receptor antagonists (D) and GABA receptor antagonists (E) in the top ranks of correlating drugs ($p = 0.031$, NMDA-R antagonists; $p = 0.034$, GABA-R antagonists; Kolmogorov-Smirnov test).

(F) Hierarchical clustering of the behavioral profiles of wild-type or *cntnap2ab* larvae exposed to 14 psychoactive agents at three doses each. Each rectangle in the clustergram represents the *Z* score relative to the behavior of wild-type or mutant larvae exposed to DMSO alone (magenta, higher than DMSO; cyan, lower than DMSO).

(G) Magnified sections highlight the behavioral fingerprints of wild-type and *cntnap2ab* larvae in response to zolpidem (20 μM).

(H) Pairwise Euclidean distances between wild-type and *cntnap2ab* responses to psychoactive agents in the PCA. Note that zolpidem and (±)-baclofen produce the strongest differential responses.

Using this approach, we found that the GABA receptor agonists zolpidem and (±)-baclofen produce the strongest differential responses of the drugs tested (Figure 3H), suggesting perturbation of GABAergic signaling pathways in mutants. Taken together, our quantitative behavioral profiling reveals dysfunction in glutamatergic as well as GABAergic pathways due to loss of Cntnap2.

Estrogens Reverse the Behavioral Phenotype of *cntnap2ab* Mutants

Next, we searched for small molecules that suppress the mutant phenotype of nighttime hyperactivity. We reasoned that such compounds might elicit a behavioral fingerprint in wild-type opposite to that of mutant larvae. We found that estrogenic compounds are significantly enriched in the top ranks of small molecules that anti-correlate with the *cntnap2ab* mutant behavioral fingerprint (Figure 4A; $p = 0.0003$ by random permutation). Specifically, four of the top ten anti-correlating drugs have known estrogenic activity. On the basis of these results, we hypothesized that such drugs might be able to rescue the mutant phenotype. To test this, we analyzed the effects of estrogenic compounds and other selected molecules in wild-type and mutant larvae using quantitative behavioral profiling and PCA (Figure 3A; see Supplemental Experimental Procedures). Behavioral rescue was defined as the shortest Euclidean distance between the mutant + drug and wild-type + no drug behavioral profiles (Figure 4D).

We found that biochanin A, a plant-derived estrogen, and β-estradiol 17-cypionate most strongly reverse the mutant behavioral phenotype (Figures 4B–4D and S4G). Indeed, the behavioral response of *cntnap2ab* larvae treated with biochanin A (0.1 μM) from 4–7 dpf most strongly correlates with the wild-type phenotype, decreasing nighttime activity with little effect on other measures of rest and activity (Figures 4B and 4C). In contrast, risperidone (0.001 μM) reverses nighttime hyperactivity but alters other rest-wake cycle parameters, indicating that it elicits a less specific phenotypic rescue than biochanin A (Figures 4C, 4E, and 4F). In addition, we found that early exposure to biochanin A does not reverse the GABAergic deficits (Figure S4M) or drug-induced seizures (Figure S4K) and that chronic exposure followed by washout does not rescue nighttime hyperactivity (Figure S4L), providing evidence for an acute mechanism of action. Consistent with estrogenic activity, we found that biochanin A (10 μM) significantly activates the expression of estrogen response genes in zebrafish larvae (Figure S4N). However, the rescue dose (1 μM) shows only a weak effect on target genes, suggesting that the behavioral rescue might occur independently of the robust transcriptional activation of estrogen target genes. Moreover, we found that biochanin A (0.1–1 μM) leads to selective suppression of nighttime activity at 5 dpf and no change in daytime activity in background-matched larvae (Figures 4G and 4H), indicating its effects are not due to background effects or generalized sedation. Furthermore, β-estradiol (1 μM) is also able to rescue nighttime hyperactivity in *cntnap2ab* mutants (Figure S4J). Together, these results provide evidence that biochanin A and β-estradiol acutely suppress a specific behavioral phenotype in a genetic loss-of-function model of an ASD risk gene.

DISCUSSION

This study represents the first characterization of zebrafish mutants of an ASD risk gene using quantitative behavioral profiling to identify biological pathways with relevance to ASDs. We demonstrate that zebrafish *cntnap2ab* mutants display reductions in GABAergic neurons, increased sensitivity to drug-induced seizures, and nighttime hyperactivity. Further, our pharmacological data support dysregulation of GABAergic and glutamatergic signaling in mutants. Altered NMDA signaling has been shown to cause GABAergic deficits, particularly in parvalbumin-positive (PV+) interneurons, and has been proposed as a mechanism underlying neuropsychiatric disorders (Keilhoff et al., 2004; Saunders et al., 2013). Moreover, mouse *Cntnap2* knockouts display GABAergic deficits, most prominently in PV+ interneurons (Peñagarikano et al., 2011). Further studies are required to determine if PV+ subpopulations are altered in *cntnap2ab* mutants, but our study highlights that GABAergic deficits are likely to occur in concert with alterations in NMDA circuits, not previously associated with Cntnap2.

Next, our results uncover the ability of estrogens to rescue the *cntnap2* mutant behavioral phenotype, suggesting that these compounds serve as modifiers of neural circuits disrupted in mutants. Indeed, estrogens can signal to multiple downstream pathways, including transcriptional activation of estrogen response genes, regulation of other transcription factors, and rapid activation of intracellular signaling pathways (Marino et al., 2006). The extent to which estrogens alter one or more downstream intracellular signaling pathways remains to be determined, but our findings suggest that the rescue activity likely involves an acute mechanism other than robust activation of estrogen target genes. Moreover, estrogens have been shown to affect glutamatergic signaling. Estradiol increases dendritic spine density and long-term potentiation via an NR2B-dependent mechanism that can be blocked by exposure to NMDA antagonists, such as MK-801 (Smith et al., 2009). Therefore, estrogens may be acting upstream of the identified NMDA and GABA deficits. Although there is growing interest in the effects of sex hormones on brain development and ASD risk, given the 4:1 male/female ratio of classical autism (Baron-Cohen et al., 2011; Schaafsma and Pfaff, 2014), further investigations are required to determine whether such a mechanism might contribute to the observed female protective effect suggested by recent human genetics studies of ASDs (Jacquemont et al., 2014).

As the list of reliable ASD risk genes continues to expand, there is a growing need for biologically relevant systems to advance from gene discovery to pharmacological screens. We demonstrate that quantitative behavioral profiling of zebrafish *cntnap2ab* mutants can be used as a novel platform for the prediction and in vivo screening of compounds to identify suppressors of a behavioral phenotype resulting from loss of an ASD risk gene. Future testing in a mammalian system is a critical next step. Moreover, the study of zebrafish mutants of the ASD risk gene, *CNTNAP2*, and its differential responses to psychoactive agents reveals the strength of this approach to identify molecular mechanisms and potential pharmacological candidates for further evaluation.

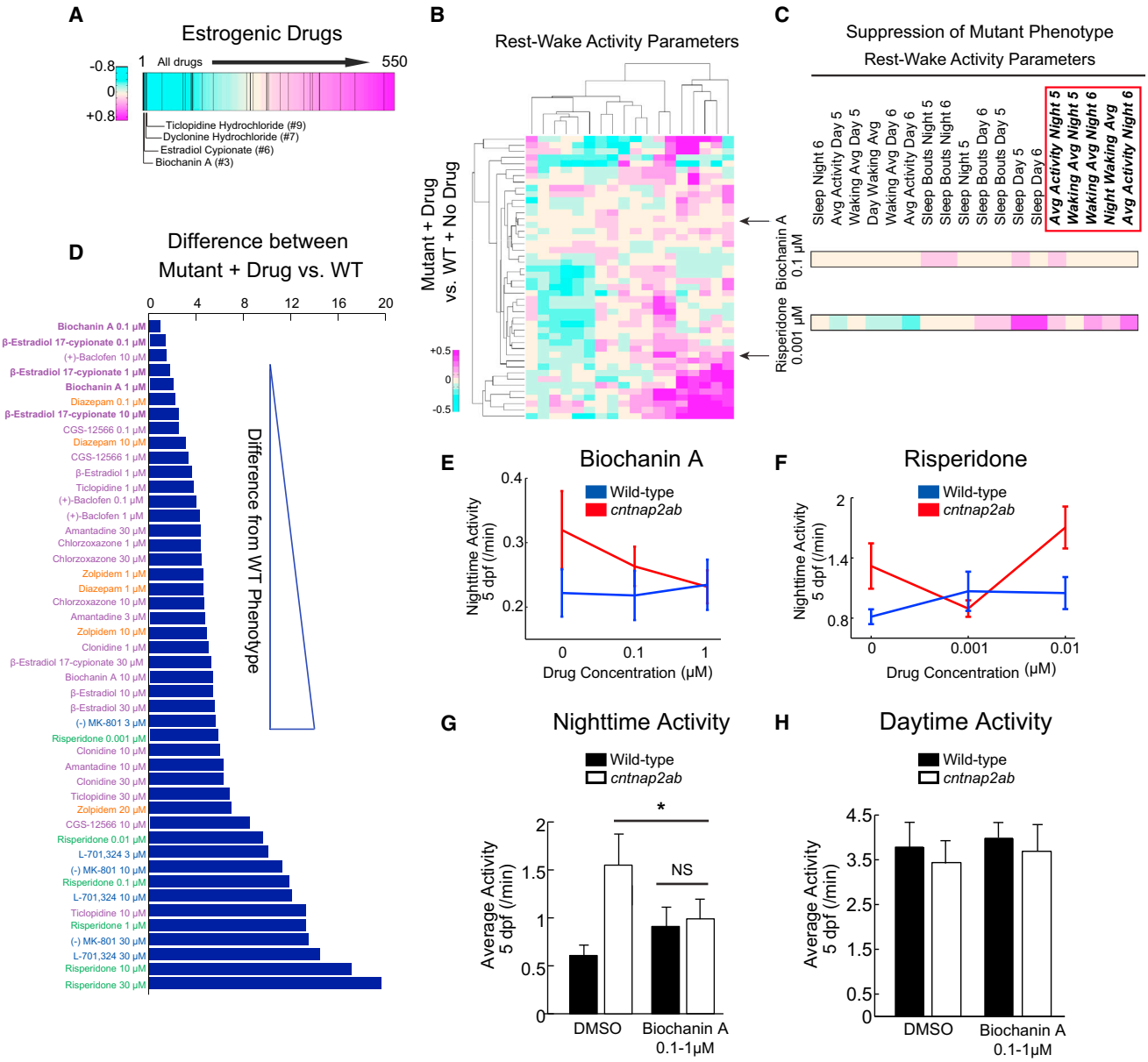

Figure 4. Biochanin A Reverses Nighttime Hyperactivity in *cntnap2ab* Mutants

(A) Rank-sorting of the anti-correlating data set with respect to estrogenic compounds shows significant enrichment of estrogenic agents in the top ranks ($p = 0.0003$ by random permutation). Black lines indicate drugs defined as having estrogenic activity (25 compounds in total).

(B) Hierarchical clustering of the behavioral fingerprints of *cntnap2a*$^{\Delta121/\Delta121}$*cntnap2b*$^{31i/31i}$ larvae exposed to 14 psychoactive agents at three doses each relative to the wild-type + no drug fingerprint. Each rectangle in the clustergram represents the *Z* score of drug-exposed mutants relative to untreated wild-type (magenta, higher than wild-type; cyan, lower than wild-type).

(C) Magnified sections of the clustergram show relative suppression of the mutant fingerprint by biochanin A (0.1 µM) compared with risperidone (0.001 µM). The red box highlights parameters that measure nighttime activity.

(D) Pairwise Euclidean distances ("Differential Drug Effects") between the mutant responses to psychoactive agents compared with untreated wild-type in the PCA (Figure S4G). Biochanin A (0.1 µM) produces the strongest suppression of the mutant phenotype in this assay, with the fewest effects on other behavioral parameters.

(E and F) Dose-response effects of biochanin A (E) and risperidone (F) on nighttime activity at 5 dpf ($p = 0.0001$, biochanin A; $p = 0.0034$, risperidone; two-way ANOVA, gene × drug interaction). Although there is some experimental variability in the baseline activity of both wild-type and mutant larvae, nighttime hyperactivity is consistently observed.

(G and H) Effect of the blind addition of biochanin A (0.1–1 µM) or DMSO on activity at night (G) and day (H) in the progeny of incrosses of *cntnap2a*$^{\Delta25/+}$*cntnap2b*$^{\Delta7/+}$ fish at 5 dpf. *$p = 0.045$ (two-way ANOVA, gene × dose interaction).

EXPERIMENTAL PROCEDURES

Zebrafish

Mutations in *cntnap2a* and *cntnap2b* were generated using zinc finger nucleases. The *cntnap2a*$^{\Delta121/\Delta121}$*cntnap2b*$^{31i/31i}$ and *cntnap2a*$^{\Delta25/\Delta25}$*cntnap2b*$^{\Delta7/\Delta7}$ lines were generated by incrossing double homozygotes, which are viable and fertile. Tg(*dlx6a-1.4kbdlx5a/dlx6a:GFP*) and Tg(*vglut:DsRed*) were obtained from the laboratories of M. Ekker and J. Fetcho, respectively. *cntnap2a*$^{\Delta121/\Delta121}$*cntnap2b*$^{31i/31i}$ mutants were crossed to these transgenic lines. Animal experiments were conducted in accordance with Institutional Animal Care and Use Committee regulatory standards (Yale University) and the UK Animals (Scientific Procedures) Act 1986.

Pharmacological Screen

Larval activity was monitored from 4–7 dpf using a custom-modified Zebrabox and automated video tracking system (Viewpoint; LifeSciences) (Rihel et al., 2010). Correlation analysis was done in MATLAB (R2014a; The MathWorks) to identify compounds that correlate or anti-correlate with the *cntnap2a*$^{\Delta25/\Delta25}$*cntnap2b*$^{\Delta7/\Delta7}$ phenotype. Three doses of each compound (Figure 3A; Table S4) were tested in 10–12 *cntnap2a*$^{\Delta121/\Delta121}$*cntnap2b*$^{31i/31i}$ or wild-type replicate larvae with 10–12 control larvae per 96-well plate (Rihel et al., 2010). Hierarchical clustering was conducted in MATLAB with the statistics and bioinformatics toolboxes.

ACCESSION NUMBERS

The accession numbers for the sequences reported in this paper are GenBank KU376408 and KU376409.

SUPPLEMENTAL INFORMATION

Supplemental Information includes Supplemental Experimental Procedures, four figures, and four tables and can be found with this article online at http://dx.doi.org/10.1016/j.neuron.2015.12.039.

AUTHOR CONTRIBUTIONS

E.J.H., M.W.S., and A.J.G. designed the project. E.J.H. generated and characterized *cntnap2ab* mutants. E.J.H. and K.J.T. performed immunohistochemistry. J.M.F. assisted in genotyping, zebrafish husbandry, and in situ hybridizations. D.C. adapted methods of mutagenesis and screening. R.A.J. and M. Granato analyzed startle and habituation. F.K. and H.B. analyzed the optokinetic response. B.R.B. provided in situ probes and discussions. E.J.H. and M.J.F.B. analyzed forebrain commissures. E.J.H., S.I., K.J.T., and S.W.W. analyzed CNS structure and GABAergic deficits. E.J.H., M. Ghosh, and J.R. performed behavioral tracking and pharmacological screens. J.R. performed correlation analyses and PCA. E.J.H. wrote the manuscript with input from S.W.W., J.R., M.W.S., and A.J.G.

ACKNOWLEDGMENTS

We thank J. Fetcho and M. Ekker for transgenic lines; B. Bill, D. Geschwind, P. Panula, and G. Wright for in situ probes; D. Geschwind, P. De Camilli, J. Leckman, M. Lee, V. Yartseva, and N. Sestan for discussions and manuscript editing; and K. Divito, J.M.F., and S. Lau (blinded raters). This work was supported by National Institutes of Health grants K08MH096176, CTSA UL1TR000142, T32MH018268, an American Academy of Child and Adolescent Psychiatry junior investigator award (E.J.H.), R21 HD073768, R01 HD074078, R01 GM081602 (A.J.G.), RC2MH089956 (A.J.G., M.W.S.), the Overlook International Foundation (M.W.S.), K99HD071968 (D.C.), MH092257 and MH109498 (M. Granato), a European Research Council Grant and University College London Excellence Fellowship (J.R.), and Biotechnology and Biological Sciences Research Council, European Union, and Wellcome Trust grants (S.W.W.).

Received: July 7, 2015
Revised: November 16, 2015
Accepted: December 21, 2015
Published: January 28, 2016

REFERENCES

Ablain, J., and Zon, L.I. (2013). Of fish and men: using zebrafish to fight human diseases. Trends Cell Biol. *23*, 584–586.

American Psychiatric Association (2013). Diagnostic and Statistical Manual of Mental Disorders, Fifth Edition (Arlington: American Psychiatric Publishing).

Baraban, S.C., Taylor, M.R., Castro, P.A., and Baier, H. (2005). Pentylenetetrazole induced changes in zebrafish behavior, neural activity and c-fos expression. Neuroscience *131*, 759–768.

Baron-Cohen, S., Lombardo, M.V., Auyeung, B., Ashwin, E., Chakrabarti, B., and Knickmeyer, R. (2011). Why are autism spectrum conditions more prevalent in males? PLoS Biol. *9*, e1001081.

Cobos, I., Calcagnotto, M.E., Vilaythong, A.J., Thwin, M.T., Noebels, J.L., Baraban, S.C., and Rubenstein, J.L. (2005). Mice lacking Dlx1 show subtype-specific loss of interneurons, reduced inhibition and epilepsy. Nat. Neurosci. *8*, 1059–1068.

De Rubeis, S., He, X., Goldberg, A.P., Poultney, C.S., Samocha, K., Cicek, A.E., Kou, Y., Liu, L., Fromer, M., Walker, S., et al.; DDD Study; Homozygosity Mapping Collaborative for Autism; UK10K Consortium (2014). Synaptic, transcriptional and chromatin genes disrupted in autism. Nature *515*, 209–215.

Ghanem, N., Jarinova, O., Amores, A., Long, Q., Hatch, G., Park, B.K., Rubenstein, J.L., and Ekker, M. (2003). Regulatory roles of conserved intergenic domains in vertebrate Dlx bigene clusters. Genome Res. *13*, 533–543.

Iossifov, I., O'Roak, B.J., Sanders, S.J., Ronemus, M., Krumm, N., Levy, D., Stessman, H.A., Witherspoon, K.T., Vives, L., Patterson, K.E., et al. (2014). The contribution of de novo coding mutations to autism spectrum disorder. Nature *515*, 216–221.

Jacquemont, S., Coe, B.P., Hersch, M., Duyzend, M.H., Krumm, N., Bergmann, S., Beckmann, J.S., Rosenfeld, J.A., and Eichler, E.E. (2014). A higher mutational burden in females supports a "female protective model" in neurodevelopmental disorders. Am. J. Hum. Genet. *94*, 415–425.

Keilhoff, G., Becker, A., Grecksch, G., Wolf, G., and Bernstein, H.G. (2004). Repeated application of ketamine to rats induces changes in the hippocampal expression of parvalbumin, neuronal nitric oxide synthase and cFOS similar to those found in human schizophrenia. Neuroscience *126*, 591–598.

Kinkhabwala, A., Riley, M., Koyama, M., Monen, J., Satou, C., Kimura, Y., Higashijima, S., and Fetcho, J. (2011). A structural and functional ground plan for neurons in the hindbrain of zebrafish. Proc. Natl. Acad. Sci. U S A *108*, 1164–1169.

Kokel, D., and Peterson, R.T. (2011). Using the zebrafish photomotor response for psychotropic drug screening. Methods Cell Biol. *105*, 517–524.

Marino, M., Galluzzo, P., and Ascenzi, P. (2006). Estrogen signaling multiple pathways to impact gene transcription. Curr. Genomics *7*, 497–508.

McCracken, J.T., McGough, J., Shah, B., Cronin, P., Hong, D., Aman, M.G., Arnold, L.E., Lindsay, R., Nash, P., Hollway, J., et al.; Research Units on Pediatric Psychopharmacology Autism Network (2002). Risperidone in children with autism and serious behavioral problems. N. Engl. J. Med. *347*, 314–321.

Parikshak, N.N., Luo, R., Zhang, A., Won, H., Lowe, J.K., Chandran, V., Horvath, S., and Geschwind, D.H. (2013). Integrative functional genomic analyses implicate specific molecular pathways and circuits in autism. Cell *155*, 1008–1021.

Peñagarikano, O., Abrahams, B.S., Herman, E.I., Winden, K.D., Gdalyahu, A., Dong, H., Sonnenblick, L.I., Gruver, R., Almajano, J., Bragin, A., et al. (2011). Absence of CNTNAP2 leads to epilepsy, neuronal migration abnormalities, and core autism-related deficits. Cell *147*, 235–246.

Poliak, S., Salomon, D., Elhanany, H., Sabanay, H., Kiernan, B., Pevny, L., Stewart, C.L., Xu, X., Chiu, S.Y., Shrager, P., et al. (2003). Juxtaparanodal clustering of Shaker-like K+ channels in myelinated axons depends on Caspr2 and TAG-1. J. Cell Biol. *162*, 1149–1160.

Prober, D.A., Rihel, J., Onah, A.A., Sung, R.J., and Schier, A.F. (2006). Hypocretin/orexin overexpression induces an insomnia-like phenotype in zebrafish. J. Neurosci. *26*, 13400–13410.

Rihel, J., Prober, D.A., Arvanites, A., Lam, K., Zimmerman, S., Jang, S., Haggarty, S.J., Kokel, D., Rubin, L.L., Peterson, R.T., and Schier, A.F. (2010). Zebrafish behavioral profiling links drugs to biological targets and rest/wake regulation. Science *327*, 348–351.

Rubenstein, J.L., and Merzenich, M.M. (2003). Model of autism: increased ratio of excitation/inhibition in key neural systems. Genes Brain Behav. *2*, 255–267.

Sanders, S.J., He, X., Willsey, A.J., Ercan-Sencicek, A.G., Samocha, K.E., Cicek, A.E., Murtha, M.T., Bal, V.H., Bishop, S.L., Dong, S., et al.; Autism Sequencing Consortium (2015). Insights into Autism Spectrum Disorder Genomic Architecture and Biology from 71 Risk Loci. Neuron *87*, 1215–1233.

Saunders, J.A., Tatard-Leitman, V.M., Suh, J., Billingslea, E.N., Roberts, T.P., and Siegel, S.J. (2013). Knockout of NMDA receptors in parvalbumin interneurons recreates autism-like phenotypes. Autism Res. *6*, 69–77.

Schaafsma, S.M., and Pfaff, D.W. (2014). Etiologies underlying sex differences in Autism Spectrum Disorders. Front. Neuroendocrinol. *35*, 255–271.

Smith, C.C., Vedder, L.C., and McMahon, L.L. (2009). Estradiol and the relationship between dendritic spines, NR2B containing NMDA receptors, and the magnitude of long-term potentiation at hippocampal CA3-CA1 synapses. Psychoneuroendocrinology *34* (*Suppl 1*), S130–S142.

Strauss, K.A., Puffenberger, E.G., Huentelman, M.J., Gottlieb, S., Dobrin, S.E., Parod, J.M., Stephan, D.A., and Morton, D.H. (2006). Recessive symptomatic focal epilepsy and mutant contactin-associated protein-like 2. N. Engl. J. Med. *354*, 1370–1377.

Watanabe, Y., Takechi, K., Fujiwara, A., and Kamei, C. (2010). Effects of antiepileptics on behavioral and electroencephalographic seizure induced by pentetrazol in mice. J. Pharmacol. Sci. *112*, 282–289.

Willsey, A.J., Sanders, S.J., Li, M., Dong, S., Tebbenkamp, A.T., Muhle, R.A., Reilly, S.K., Lin, L., Fertuzinhos, S., Miller, J.A., et al. (2013). Coexpression networks implicate human midfetal deep cortical projection neurons in the pathogenesis of autism. Cell *155*, 997–1007.

Zerucha, T., Stühmer, T., Hatch, G., Park, B.K., Long, Q., Yu, G., Gambarotta, A., Schultz, J.R., Rubenstein, J.L., and Ekker, M. (2000). A highly conserved enhancer in the Dlx5/Dlx6 intergenic region is the site of cross-regulatory interactions between Dlx genes in the embryonic forebrain. J. Neurosci. *20*, 709–721.